

On the Performance of Spectrally-Encoded Spread-Time Ultrawideband CDMA Communication Systems

Mahmoud Farhang, *Student Member, IEEE*, and Jawad A. Salehi, *Senior Member, IEEE*

Abstract—In this paper we study the performance of Spectrally-Encoded Spread-Time (SE/ST) technique when applied to ultrawideband (UWB) signals in the context of wireless code-division multiple-access (CDMA) communication. In this technique UWB pulses are spectrally encoded with pseudo-random codes that are assigned uniquely to each user. We shall show that the SE/ST ultrawideband system provides an appropriate multi-user capacity in realistic UWB channels, along with the ability of narrowband interference (NBI) suppression. To this end, after obtaining a suitable statistical model for spectrally-encoded spread-time signals, we investigate the performance of the system in the presence of multiple-access and narrowband interferers, and simple and accurate approximations will also be developed which are in good agreement with simulation results. Furthermore, the effect of variations of the main system parameters and some of the relevant trade-offs will be numerically demonstrated.

Index Terms—Spread-time, code-division multiple-access, ultrawideband, multiple-access interference, narrowband interference.

I. INTRODUCTION

EVER since the approval for the deployment of ultrawideband (UWB) on an unlicensed basis by Federal Communications Commission (FCC), it is emerging as a solution for low-complexity high data rate wireless communications in a short range environment. To allow multiple users share this invaluable resource in an asynchronous and decentralized manner, the use of code-division multiple-access (CDMA) techniques seems to be a viable approach [1]-[3].

Besides the conventional CDMA techniques, such as time-hopping (TH) or direct-sequence (DS), spectrally-encoded spread-time (SE/ST) CDMA technique could also be considered as a promising alternative for impulse radio UWB communications [4]-[6]. This technique can be thought of as the time-frequency dual of direct-sequence spread-spectrum technique; multiplying a PN sequence to the spectrum of an ultrawideband pulse spreads the energy of the pulse in time domain, just as applying a PN sequence to a pulse in time domain spreads its energy in frequency domain. The inherent flexibility in spectral shaping and spectrum management in

Manuscript received June 12, 2007; revised March 6, 2008; accepted April 5, 2008. The associate editor coordinating the review of this paper and approving it for publication was S. Hanly. Part of this paper was supported by the Iran National Science Foundation (INSF).

The authors are with the Optical Networks Research Lab, Department of Electrical Engineering, Sharif University of Technology, Tehran, Iran (e-mail: farhang@ee.sharif.edu, jasalehi@sharif.edu).

Digital Object Identifier 10.1109/T-WC.2008.070633

SE/ST is an efficient solution in alleviating narrowband interferences (NBI) which can severely deteriorate the performance of UWB communication systems [7],[8].

The concept of spectral coding of ultrawideband pulses was first proposed in the context of optical CDMA communications systems [9] and then was extended to wireless CDMA communications systems [10]. The performance of this technique has been studied in some special cases before. In [10] the performance of the multiple access system in an AWGN channel is evaluated. In [4] a fading channel is assumed, but only the average signal to interference plus noise ratio is evaluated which clearly is not a suitable criterion for digital communication systems. Finally, in [6] the authors have examined the performance in a single user UWB scenario in the presence of narrowband interference.

In this paper we shall investigate the performance of an UWB SE/ST system in the presence of multi-user and narrowband interferences. It turns out that the exact evaluation of probability of error cannot be performed analytically and instead we obtain simple accurate approximations for the performance and justify them numerically through Monte-Carlo simulations.

The rest of this paper is organized as follows. In section II we briefly describe SE/ST UWB CDMA and study the statistical characteristics of the spectrally encoded signals. In section III its multiple-access performance in UWB channels is studied. Narrowband interference mitigation capability of spectrally-encoded spread-time UWB CDMA is treated in section IV, and in section V some numerical results are presented. Section VI concludes the paper.

II. SPECTRALLY-ENCODED SPREAD-TIME UWB CDMA

A. System Description

Fig. 1 and Fig. 2 show simplified block diagrams of a transmitter and receiver pair of a SE/ST UWB system. The ultrawideband data modulated pulses to be transmitted are spectrally encoded by a pseudo-random sequence which is uniquely assigned to each user, and as a result of this spectral slicing and encoding, the input pulses are spread in time. At the receiver by applying the complex conjugate of the same spectral code to the time spread signal the original ultrashort pulse will be recovered, while signals of other users -which are spread by different pseudo-random codes- will remain spread in time.

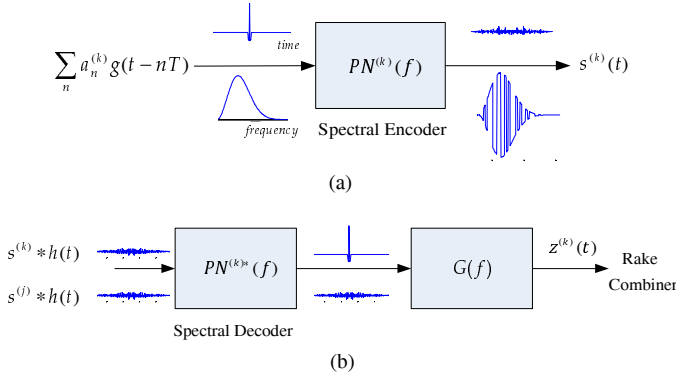


Fig. 1. (a) SE/ST-UWB transmitter, and (b) SE/ST-UWB receiver

Specifically, let $\sum_n a_n^{(k)} g(t - nT)$ be the input signal to the spectral encoder of the k th user, in which $g(t)$ is the UWB pulse and $\{a_n^{(k)}\}$ is the data sequence. In the following a BPSK modulation will be assumed. From Fig. 1 the output of the spectral encoder can be written as

$$s^{(k)}(t) = \sum_n a_n^{(k)} p^{(k)}(t - nT), \quad (1)$$

where $p^{(k)}(t) = g(t) * pn^{(k)}(t)$, with $pn^{(k)}(t)$ being the inverse Fourier transform of the spectral code $PN^{(k)}(f)$.

Let $2W$ denote the total signal bandwidth, and assume $PN^{(k)}(f)$ has the same frequency support as the ultrawideband pulse, and consists of chips that are Ω Hz wide (Fig. 3), and let $N_0 = \frac{2W}{\Omega}$, therefore

$$PN^{(k)}(f) = \sum_{m=0}^{N_0/2-1} c_m^{(k)} r_\Omega(f - f_L - m\Omega), f > 0 \quad (2)$$

with $\{c_i^{(k)}\}$ being the pseudo-random spectral code of user k , $r_\Omega(f) = \begin{cases} 1 & 0 < f < \Omega \\ 0 & \text{o.w.} \end{cases}$, and $PN^{(k)}(-f) = PN^{(k)*}(f)$ to render the signal real. f_L is the lower cutoff frequency of the UWB pulse, and for simplicity is taken to be zero in the following. So, the transmitted spectrally coded pulse will be,

$$p^{(k)}(t) = g(t) * \underbrace{\left(\frac{\sin \pi \Omega t}{\pi t} \sum_{m=-N_0/2}^{N_0/2-1} c_m^{(k)} e^{j2\pi \Omega(m+1/2)t} \right)}_{pn^{(k)}(t)}. \quad (3)$$

The temporal width of the term in the parenthesis is determined by its envelope, i.e., $\frac{\sin \pi \Omega t}{\pi t}$, and approximately equals $\frac{2}{\Omega} = \frac{N_0}{W}$. As the duration of $g(t)$ is on the order of $\frac{1}{W}$, for $N_0 \gg 1$ the time duration of $p^{(k)}(t)$ is approximately $\frac{N_0}{W}$, from which the resulting time spreading is clear. Also, from (3) it is seen that the coded pulse is of infinite duration, and thus it must be truncated by a proper time window $w(t)$. It is shown in [11] that windowing has a negligible effect on the performance, so for simplicity we consider $w(t) = 1, \forall t$, in our analysis.

B. Statistical Analysis of the Encoded Signal

In this subsection we study and analyze the statistical properties of the encoded, or equivalently, incorrectly decoded

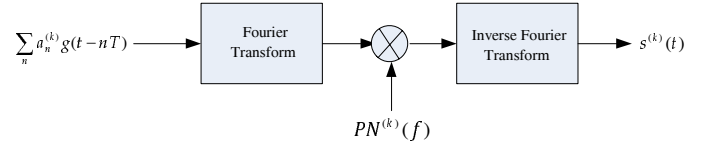


Fig. 2. Spectral encoder implementation using Fourier transformers

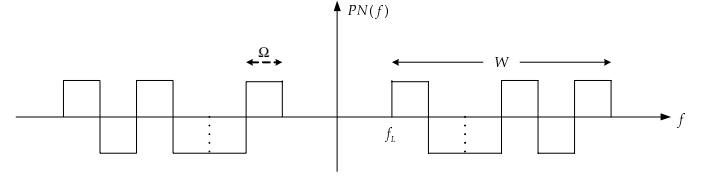


Fig. 3. An example of a spectral pseudo-random code

signals which constitute the multiple access interference at the receiver.

The statistics of single spectrally coded pulses has already been analyzed in the context of the optical counterpart of the SE/ST-CDMA technique [9], and the results can be reproduced here with minor modifications. However, as we shall see, our desired model should consider the spread-time pulse train as a whole and such a model has not been developed before.

If (pseudo) random, zero mean spectral codes of sufficiently large length are assumed ($N_0 \gg 1$), then by invoking the multivariate central-limit theorem ([9],[13]) one can easily show that $p^{(k)}(t)$ is a zero mean nonstationary Gaussian random process [c.f. (3)]. Therefore, the pulse train $\sum_n a_n^{(k)} p^{(k)}(t - nT)$ will also be a zero mean Gaussian random process. In Appendix A the autocorrelation function of this process is derived, and it is shown that if $\{a_n^{(k)}\}$ are equiprobable ± 1 , and if $c_i^{(k)} = e^{jn_i \pi/2}$, where n_i takes on values 0, 1, 2 or 3 with equal probability, then we have

$$\begin{aligned} \mathbb{E}\{s^{(k)}(t)s^{(k)}(t+\tau)\} &= \frac{1}{T} \int |G(f)|^2 e^{-j2\pi f \tau} df \\ &+ \frac{1}{T} \sum_{n=1}^{\lfloor T\Omega \rfloor} \cos\left[\frac{2\pi n}{T}(t + \frac{\tau}{2})\right]. \\ \mathcal{F}_\tau^{-1}\{G(f + \frac{n}{2T})G(f - \frac{n}{2T})\} &* \left(\frac{\sin(\Omega - n/T)\pi\tau}{\pi\tau} \frac{\sin N_0\Omega\pi\tau}{\sin \Omega\pi\tau} \right) \end{aligned} \quad (4)$$

where $\lfloor x \rfloor$ is the integer part of x and $\mathcal{F}_\tau^{-1}\{\cdot\}$ denotes the inverse Fourier transform with τ as the argument. Thus, if the product of the width of the frequency chip and the bit period is less than one ($T\Omega < 1$), that is, when adjacent coded pulses have a considerable amount of overlapping ($T < T_{cp}/2$, with $T_{cp} \approx N_0/W$ being the duration of the coded pulse), the encoded (or incorrectly decoded) signal becomes a stationary process. Moreover, it is not difficult to verify that the right hand side of (4) becomes negligible for $\tau \geq \frac{1}{W}$ and hence samples of the coded signal which are apart by more than this value are nearly uncorrelated.

III. MULTIPLE-ACCESS PERFORMANCE OF SPECTRALLY-ENCODED SPREAD-TIME UWB CDMA

In this section we analyze the performance of a general spectrally-encoded spread-time multi-user system taking into account the indoor channel model for UWB communications.

A. Multipath Channel Model and Rake Receiver

The channel that we use here is the widely used indoor UWB channel model, in which the multipath channel is modeled as a finite impulse response filter

$$h(t) = \sum_{i=1}^{L_p} \alpha_i \delta(t - \tau_i) \quad (5)$$

where L_p is the number of multipath components, and α_i and τ_i are the amplitude and delay of the i th path, respectively [14]-[16]. With the common assumption of resolvable multipath components, that is $|\tau_l - \tau_{l-1}| \geq T_p$, where T_p is the time width of the pulse, the delays can be written as $\tau_i = \tau_1 + (i-1)T_p$. The arrival time of the first multipath component is assumed to have a uniform distribution in $[0, T]$. Also, the multipath gains can be expressed as $\alpha_i = b_i |\alpha_i|$, with b_i being equiprobable ± 1 to account for the signal inversion due to reflections, and $|\alpha_i|$ is modeled as a Nakagami random variable with an exponential power decay profile [14]-[16].

If we neglect the effect of the antenna on the pulse shape, the signal at the input of the spectral decoder of the desired user's receiver, e.g., user 1, can be written as

$$\begin{aligned} r^{(1)}(t) = & \sum_n a_n^{(1)} \sum_{i=1}^{L_p^{(1)}} \alpha_i^{(1)} p^{(1)}(t - nT - \tau_i^{(1)}) \\ & + \sum_{j=2}^K \sum_n a_n^{(j)} \sum_{i=1}^{L_p^{(j)}} \alpha_i^{(j)} p^{(j)}(t - nT - \tau_i^{(j)}) + n(t) \end{aligned} \quad (6)$$

K is the number of active users, $n(t)$ is an AWGN with two sided power spectral density $\eta/2$, and $L_p^{(j)}$, $\alpha_p^{(j)}$ and $\tau_p^{(j)}$ are the parameters of the channel between the transmitter of user j and the receiver of user 1.

The signal in (6) after passing through the spectral decoder and matched filter can be expressed as [c.f. Fig. 1.(b)]

$$\begin{aligned} z^{(1)}(t) = & \sum_n a_n^{(1)} \sum_{i=1}^{L_p^{(1)}} \alpha_i^{(1)} (g * g)(t - nT - \tau_i^{(1)}) \\ & + \sum_{j=2}^K \sum_n a_n^{(j)} \sum_{i=1}^{L_p^{(j)}} \alpha_i^{(j)} \tilde{p}^{(j)}(t - nT - \tau_i^{(j)}) + \tilde{n}(t) \end{aligned} \quad (7)$$

where $\tilde{p}^{(j)}(t)$ is the response of the receiver's spectral decoder and matched filter to $p^{(j)}(t)$, that is, $\tilde{P}^{(j)}(f) = PN^{(j)}(f)PN^{(1)*}(f)|G(f)|^2$, and $\tilde{n}(t)$ is the filtered noise with power spectral density $\frac{\eta}{2}|G(f)|^2$. It is clear from (7) that the transmitted energy is dispersed over many multipath components, so a Rake receiver is needed to boost the output SNR [18]. Since the number of resolvable paths is usually high, a *Selective Rake* (SRake) receiver which trades off complexity against performance may be used [19]. This receiver diversity combines the strongest L paths and is optimum among all Rake receivers that have only L fingers. An SRake receiver, however, needs a selection mechanism that estimates the power of all paths and selects the strongest ones. It can be shown that a *Partially Rake* (PRake) receiver which

combines the *first* L paths has a comparable performance with an SRake receive in realistic UWB channels, but with much less complexity [20],[21].

So in our analysis we choose a PRake receiver with the optimal combining scheme, i.e., maximal ratio combining (MRC) [18]. This receiver can be implemented simply by passing the output of the matched filter [eq. (7)] through a tapped delay line with delays and tap coefficients being equal to the corresponding estimated delays and coefficients from the channel, and then combining them together.

B. Performance Analysis

Let $y(t)$ denote the output of the PRake receiver with MRC, assuming perfect synchronization and channel estimation. Its sample at $t = mT$ is the statistics on which the decision regarding a_m is based [18]

$$\begin{aligned} y(mT) = & a_m^{(1)} E_0 \sum_{l=1}^L (\alpha_l^{(1)})^2 \\ & + \sum_{n, n \neq m} a_n \sum_{l=1}^L \sum_{i=1}^{L_p^{(1)}} \alpha_l^{(1)} \alpha_i^{(1)} (g * g)((m-n)T + \tau_l^{(1)} - \tau_i^{(1)}) \\ & + \sum_{j=2}^K \sum_n \sum_{l=1}^L \sum_{i=1}^{L_p^{(j)}} a_n^{(j)} \alpha_l^{(1)} \alpha_i^{(j)} \tilde{p}^{(j)}((m-n)T + \tau_l^{(1)} - \tau_i^{(j)}) \\ & + \sum_{l=1}^L \alpha_l^{(1)} \tilde{n}_{ml} \end{aligned} \quad (8)$$

with the decision rule: $y(mT) \stackrel{a_m = -1}{\underset{a_m = +1}{\leq}} 0$. In (8) \tilde{n}_{ml} is the sample of the filtered noise at $t = mT + \tau_l^{(1)}$, and $E_0 = (g * g)(0) = \int |G(f)|^2 df$.

The terms in (8) correspond to the desired signal, inter-symbol interference (ISI), multiple access interference (MAI), and additive noise, respectively. The amount of ISI in an SE/ST-UWB system in which only one pulse per symbol is transmitted and the interpulse interval is much larger than the pulse width can be very small. Hence in the following we will neglect the ISI terms. However, in severe channel conditions and/or very high data rates, where ISI becomes an important limiting factor, a post-Rake equalizer can be used to remove the introduced ISI [18]. So by dispensing with ISI terms, the decision statistics reduces to

$$\begin{aligned} y(mT) = & a_m^{(1)} s_m + i_m + n_m \\ = & a_m^{(1)} E_0 \|\alpha^{(1)}\|^2 + \sum_{j=2}^K \sum_n a_n^{(j)} \alpha^{(1)T} \tilde{\mathbf{P}}_{m,n}^{(j)} \alpha^{(j)} \\ & + \alpha^{(1)T} \tilde{\mathbf{n}}_m \end{aligned} \quad (9)$$

where $\alpha^{(1)} = [\alpha_1^{(1)} \dots \alpha_L^{(1)}]^T$, $\alpha^{(j)} = [\alpha_1^{(j)} \dots \alpha_{L_p^{(j)}}^{(j)}]^T$, $\tilde{\mathbf{n}}_m = [\tilde{n}_{m1} \dots \tilde{n}_{mL}]^T$, and $\tilde{\mathbf{P}}_{m,n}^{(j)}$ is an $L \times L_p^{(j)}$ matrix with $[\tilde{\mathbf{P}}_{m,n}^{(j)}]_{l,i} = \tilde{p}^{(j)}((m-n)T + \tau_l^{(1)} - \tau_i^{(j)})$. The norm of a vector $\alpha = [\alpha_1 \dots \alpha_N]^T$ is defined as $\|\alpha\| = \sqrt{\alpha_1^2 + \dots + \alpha_N^2}$. It should be noted that in general channel parameters may vary with time. Nonetheless, for applications at pedestrian

speeds or slower -which are typical of indoor applications- the time variations of the channel are very slow [17], and the multipath parameters will stay unchanged for many symbol periods (quasi-stationary approximation).

To evaluate the performance of the system, we first obtain the probability distribution of the second and third terms in (9), conditioned on channel parameters. The third term is a weighted sum of samples of the filtered noise, which by the assumption of sufficiently separated samples, i.e., resolvable multipath components, will remain uncorrelated. So it is a zero mean Gaussian random variable with a variance $\sigma_n^2 = \|\alpha^{(1)}\|^2 \sigma_n^2 = \frac{\eta}{2} \|\alpha^{(1)}\|^2 \int |G(f)|^2 df$.

Following the discussion in II.B, the MAI term i_m in (9) is a summation of zero mean Gaussian random variables and it will also be a zero mean Gaussian random variable. Noting that $\mathbb{E}\{a_m^{(j)} a_n^{(k)}\} = \delta_{mn} \delta_{jk}$, its variance conditioned on channel parameters can be written as

$$\begin{aligned} \sigma_i^2 &\triangleq \mathbb{E}\{i_m^2 | \alpha, \tau\} = \mathbb{E}\left\{\left(\sum_{j=2}^K \sum_n a_n^{(j)} \alpha^{(1)T} \tilde{\mathbf{P}}_{m,n}^{(j)} \alpha^{(j)}\right)^2 | \alpha, \tau\right\} \\ &= \sum_{j=2}^K \sum_n \mathbb{E}\left\{\left(\alpha^{(1)T} \tilde{\mathbf{P}}_{m,n}^{(j)} \alpha^{(j)}\right)^2 | \alpha, \tau\right\} \\ &= \sum_{j=2}^K \sum_{l=1}^L \sum_{i=1}^{L_p^{(j)}} \sum_{l'=1}^L \sum_{i'=1}^{L_p^{(j)}} \alpha_l^{(1)} \alpha_{i'}^{(j)} \alpha_{l'}^{(1)} \alpha_{i'}^{(j)} \\ &\quad \mathbb{E}\left\{\sum_n \tilde{p}^{(j)}((m-n)T + \tau_l^{(1)} - \tau_{i'}^{(j)}) \right. \\ &\quad \left. \tilde{p}^{(j)}((m-n)T + \tau_{l'}^{(1)} - \tau_{i'}^{(j)}) | \tau\right\} \end{aligned} \quad (10)$$

in which $\alpha = \{\alpha^{(1)T}, \dots, \alpha^{(K)T}\}$ and $\tau = \{\tau_1^{(1)}, \tau_1^{(2)}, \dots, \tau_1^{(K)}\}$.

Since $\tilde{p}^{(j)}(t)$ is the output of a matched filter with frequency response $PN^{(1)*}(f)G^*(f)$ for the input $p^{(j)}(t)$, and since the product $PN^{(j)}(f)PN^{(1)*}(f)$ is another pseudo-random spectral code, the expectation in the right hand side of (10) can be readily obtained from (4) [c.f. (27)], in which $G(f)$ is replaced by $|G(f)|^2$:

$$\begin{aligned} \mathbb{E}\left\{\sum_n \tilde{p}^{(j)}(t-nT) \tilde{p}^{(j)*}(t+\tau-nT)\right\} &= \\ \frac{1}{T} \int |G(f)|^4 e^{-j2\pi f \tau} df + \\ \frac{2}{T} \sum_{n=1}^{\lfloor T\Omega \rfloor} \cos\left[\frac{2\pi n}{T}(t+\frac{\tau}{2})\right] \int \left|G\left(f+\frac{n}{2T}\right)G\left(f-\frac{n}{2T}\right)\right|^2 &(11) \\ \sum_{k=-N_0/2}^{N_0/2-1} r_{\Omega-\frac{\pi}{T}}\left(f-\frac{n}{2T}-k\Omega\right) e^{-j2\pi f \tau} df \end{aligned}$$

Therefore the conditional probability of error for BPSK modulation with equiprobable data is given by $P_{e|\alpha, \tau} = Q(\sqrt{SINR})$, $SINR = \frac{\sigma_m^2}{\sigma_i^2 + \sigma_n^2}$, and the probability of error is obtained by averaging $P_{e|\alpha, \tau}$ over α, τ :

$$P_e = \mathbb{E}_{\alpha, \tau}\{Q(\sqrt{SINR})\} \quad (12)$$

The above expectation cannot be put into simple analytical forms and should be evaluated using semi-analytical proce-

dures, i.e., averaging $P_{e|\alpha, \tau}$ over many channel realizations via simulation [22]. However, in the next subsection we obtain a simple and accurate approximation to this expression which is in good agreement with simulation results presented in section V.

C. Performance Approximation

The expectation in (12) is encountered quite often in the performance analysis of CDMA communication systems and since almost always it cannot be dealt with analytically, a number of techniques have been so far developed to obtain accurate approximations for the performance. One of the most simple and accurate of these methods is the following approximation for the expected value of a function $p(\cdot)$ of a random variable x [24]-[26]:

$$\mathbb{E}\{p(x)\} \approx \frac{2}{3}p(\mu_x) + \frac{1}{6}p(\mu_x + \sqrt{3}\sigma_x) + \frac{1}{6}p(\mu_x - \sqrt{3}\sigma_x) \quad (13)$$

where μ_x and σ_x^2 are the mean and variance of the random variable x . With the assumption of a slowly time-varying channel and a perfect power control mechanism, we can neglect the effect of variations of the received signal energy on the performance. Hence, with $p(x) = Q(\sqrt{\frac{s_m^2}{x}})$, $x = \sigma_i^2 + \sigma_n^2$, from (12) and (13) we have

$$\begin{aligned} P_e &\approx \frac{2}{3}Q\left(\sqrt{\frac{s_m^2}{\mu_x}}\right) + \frac{1}{6}Q\left(\sqrt{\frac{s_m^2}{\mu_x + \sqrt{3}\sigma_x}}\right) \\ &\quad + \frac{1}{6}Q\left(\sqrt{\frac{s_m^2}{\max\{\mu_x - \sqrt{3}\sigma_x, 0\}}}\right) \end{aligned} \quad (14)$$

where μ_x and σ_x^2 are given by (Appendix B)

$$\mu_x = \mathbb{E}\{\|\alpha^{(1)}\|^2\} \sum_{j=2}^K \mathbb{E}\{\|\alpha^{(j)}\|^2\} \gamma_1 + \mathbb{E}\{\|\alpha^{(1)}\|^2\} \sigma_n^2 \quad (15)$$

$$\begin{aligned} \sigma_x^2 &= 2 \sum_{l, l'=1, l' \neq l}^L \mathbb{E}\{|\alpha_l^{(1)}|^2 |\alpha_{l'}^{(1)}|^2\} \sum_{j=2}^K \sum_{i=1}^{L_p^{(j)}} \mathbb{E}\{|\alpha_i^{(j)}|^2 |\alpha_{i+l-l}^{(j)}|^2\} \gamma_2^2 \\ &\quad + \left(\mathbb{E}\{\|\alpha^{(1)}\|^4\} - \mathbb{E}^2\{\|\alpha^{(1)}\|^2\}\right) \cdot \\ &\quad \left(\sigma_n^4 + 2\sigma_n^2 \sum_{j=2}^K \mathbb{E}\{\|\alpha^{(j)}\|^2\} \gamma_1\right) \end{aligned} \quad (16)$$

In the above expressions $\gamma_1 = \frac{1}{T} \int |G(f)|^4 df$, $\sigma_n^2 = \frac{\eta}{2} \int |G(f)|^2 df$, and

$$\begin{aligned} \gamma_2^2 &= \left(\frac{1}{T} \int |G(f)|^4 df\right)^2 + \frac{2}{T^2} \sum_{n=1}^{\lfloor T\Omega \rfloor} \\ &\quad \left(\sum_{k=-N_0/2}^{N_0/2-1} \int_{k\Omega+\frac{n}{2T}}^{(k+1)\Omega-\frac{n}{2T}} \left|G\left(f+\frac{n}{2T}\right)G\left(f-\frac{n}{2T}\right)\right|^2 df\right)^2. \end{aligned}$$

It also should be noted that the accuracy of the approximation in (13) is very high if x has a normal distribution [27]. Indeed, by using a generalized version of the central-limit theorem for m-dependent random variables [28] it can be shown that for sufficiently large L , σ_i^2 as defined in (10) approaches a Gaussian random variable in distribution, hence improving the validity of (13). Moreover, the simulation results in section V justify the accuracy of this approximation.

IV. NARROW-BAND INTERFERENCE MITIGATION

Coexistence with other narrowband systems is one of the major challenges of UWB technology. Although the imposed power spectral density (PSD) mask for UWB transmissions by FCC guarantees intangible interference from UWB devices to other narrowband systems [23], the interference from nearby narrowband systems on UWB devices could degrade their performance severely [7],[8]. The usual low duty cycle of UWB transmissions brings a processing gain on the order of T/T_p , where T is the period of transmission and T_p is the pulse width. But in many high data rate applications, when nearby interferers or intended jammers also exist, the above processing gain cannot be relied on. Furthermore, multiple-access techniques like TH or DS essentially cannot improve the processing gain beyond the processing gain given to achieve multiple-access capability.

The flexibility in spectrum shaping in spectrally-encoded ST technique makes it possible to dynamically suppress strong narrowband interferences when they are sensed. When this is the case in some frequency chips, the amplitude of their spectral code can be set to zero.

In this section we examine the capability of spectrally-encoded spread-time UWB CDMA in combating narrowband interferences. This feature of ST technique has been previously demonstrated in [6] for a single user system semi-analytically.

Consider a multi-user system in which a zero mean stationary Gaussian partial band jammer $J(t)$ with power spectral density $S_J(f)$ is present. The output of the PRake receiver with MRC at time $t = mT$ will be [c.f. (9)]

$$y(mT) = s_m + i_m + j_m + n_m \quad (17)$$

s_m , i_m , and n_m are as in (9), and the narrowband interference term is given by

$$j_m = \sum_{l=1}^L \alpha_l^{(1)} \tilde{J}(mT - \tau_l) \quad (18)$$

where $\tilde{J}(t)$ is the filtered NBI [c.f. (7)]. Thus the BER with the interference being present will be

$$P_{e1} = \mathbb{E}_{\alpha, \tau} \left\{ Q \left(\sqrt{\frac{s_m^2}{\mathbb{E}\{j_m^2 | \alpha^{(1)}\} + \sigma_i^2 + \sigma_n^2}} \right) \right\} \quad (19)$$

With $R_{\tilde{J}}(\tau) = \mathcal{F}_\tau^{-1} \{ S_J(f) |G(f)|^2 \}$ being the autocorrelation function of $\tilde{J}(t)$, the interference power can be expressed as

$$\mathbb{E}\{j_m^2 | \alpha^{(1)}\} = \sum_{l=1}^L \sum_{l'=1}^L \alpha_l^{(1)} \alpha_{l'}^{(1)} R_{\tilde{J}}(\tau_l - \tau_{l'}) \quad (20)$$

After interference suppression by assigning the level zero to the interfered chips, the BER becomes

$$P_{e2} = \mathbb{E}_{\alpha, \tau} \left\{ Q \left(\sqrt{\frac{\hat{s}_m^2}{\hat{\sigma}_i^2 + \hat{\sigma}_n^2}} \right) \right\} \quad (21)$$

where ‘ $\hat{\cdot}$ ’ denotes the removal of the contaminated spectral chips in the evaluation of the desired value, i.e., $\hat{s}_m = \|\alpha\|^2 \left(\int_{-\infty}^{\infty} |G(f)|^2 df - \int_{\mathcal{A}} |G(f)|^2 df \right)$, etc., with \mathcal{A} being the frequency support of $S_J(f)$.

As was the case in section III.B, the exact evaluation of (19) and (21) is not tractable. Nevertheless, along the same lines of the previous section and by using the approximation (13), P_{e1} and P_{e2} could be easily estimated. In the case of P_{e1} , $p(x_1) = Q(\sqrt{s_m^2/x_1})$, $x_1 = \mathbb{E}\{j_m^2 | \alpha^{(1)}\} + \sigma_i^2 + \sigma_n^2$. Therefore, $\mu_{x1} = \mu_x + \mathbb{E}\{\|\alpha^{(1)}\|^2\} \sigma_j^2$ with μ_x as in (15) and $\sigma_j^2 = R_{\tilde{J}}(0)$. With σ_x^2 as in (16), we have (Appendix B)

$$\begin{aligned} \sigma_{x1}^2 &= \sigma_x^2 + \sigma_j^2 \left(\mathbb{E}\{\|\alpha^{(1)}\|^4\} - \mathbb{E}^2\{\|\alpha^{(1)}\|^2\} \right) \\ &\quad \left(\sigma_j^2 + 2 \sum_{j=2}^K \mathbb{E}\{\|\alpha^{(j)}\|^2\} \cdot \gamma_1 + \sigma_n^2 \right) \\ &\quad + 2 \sum_{l, l'=1, l' \neq l}^L \mathbb{E}\{|\alpha_l^{(1)}|^2 |\alpha_{l'}^{(1)}|^2\} R_{\tilde{J}}^2(\tau_l - \tau_{l'}) \end{aligned} \quad (22)$$

For P_{e2} , $p(x_2) = Q(\sqrt{\hat{s}_m^2/x_2})$, $x_2 = \hat{\sigma}_i^2 + \hat{\sigma}_n^2$, and it easily follows that $\mu_{x2} = \hat{\mu}_x$ and $\sigma_{x2}^2 = \hat{\sigma}_x^2$.

The simulation results in the next section confirm the accuracy of the above approximations and manifest this NBI suppression capability of SE/ST-CDMA. Some of the related trade-offs are also investigate.

V. NUMERICAL RESULTS

The conditional BER expressions attained in sections III and IV are evaluated in this section by semi-analytical methods (Monte-Carlo simulations) to assess an estimate of the system performance in different scenarios, and also to demonstrate the accuracy of the invoked approximations. To this end, we consider the channel model (5), in which $|\alpha_i|$ has a Nakagami distribution with parameter m_i and average power $\mathbb{E}\{\alpha_i^2\}$, and due to the exponential power decay model $\mathbb{E}\{\alpha_i^2\} = \mathbb{E}\{\alpha_1^2\} e^{-\varepsilon(\tau_i - \tau_1)}$. The power decay constant ε and the parameter m_i are in general random variables, but to simplify the analysis and simulation were kept fixed to their mean value [16], [21]. The average total channel gain is also normalized to unity, i.e., $\mathbb{E}\{\sum \alpha_i^2\} = 1$. Generalizations to more realistic channel conditions are straightforward.

In all the following numerical examples we have chosen $L = 25$, $\varepsilon = 0.3$, and $m = 3$. The pulse shape is considered to be a Gaussian monocycle ($G(f) = Af^2 \exp(-f^2 \sigma^2)$) with a -10 dB bandwidth W and $\text{SNR} = E_0/\eta$ is set at 15 dB.

A. Multiple Access Performance

The main parameters affecting the multi-access performance of the system are the code length N_0 and the bit time to pulse width ratio (or the product TW). Fig. 4 shows the performance for some different values of TW and the spectral code length (or equivalently $T\Omega$), versus the number of simultaneous users K , with the assumption of identical channel parameters for all users. Both the analytical evaluation using approximation (14) and simulation results are presented, whence the high accuracy of the approximation, for K not being too small (i.e., $K \geq 4$), is evident. For $TW = 16$ only the results of $N_0 = 32$ are plotted, as the Gaussian assumption for the multi-user interference may not have the sufficient accuracy for $N_0 < 32$. We also note that, as in any other CDMA system, given a bandwidth W there exists a trade-off between the multi-user capacity and the bit rate. Moreover, we observe

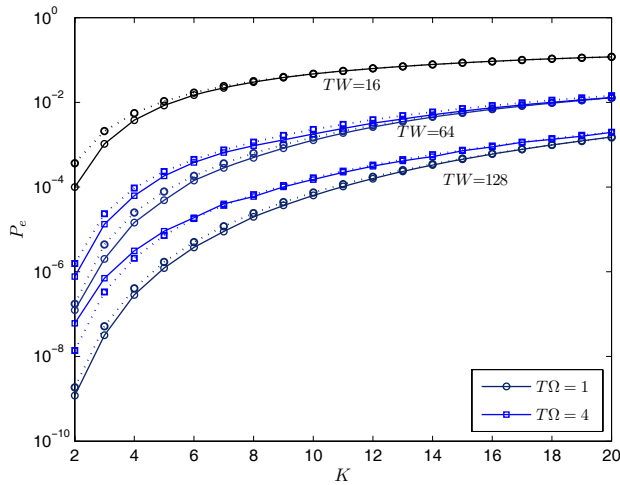


Fig. 4. Performance of the SE/ST CDMA technique versus number of simultaneous users for different time-bandwidth products and spectral code lengths. Solid lines: Monte-Carlo simulation, dotted lines: approximation

that although an increase in N_0 improves the performance to some extent, it may not counterbalance the added complexity to the spectral encoder and decoder, especially as K gets large.

If the code length is increased, the pulse temporally spreads in a longer duration and as a result, we may expect that the level of the multi-access interference would be lowered. With TW held fixed, however, the above statement is true unless contiguous pulses do not overlap significantly after the spectral encoding. This overlapping, on the other hand, would raise the interference power, and increasing N_0 beyond a certain limit does not improve the performance anymore. In Fig. 5 we demonstrate how variations of N_0 and TW have different effects on the system performance for a fixed number of simultaneous users ($K = 8$). We note that while increasing the bit period-bandwidth product continuously improves the performance, the matter is not the same for N_0 . In fact the increase in N_0 will reduce the interference power unless $T\Omega < 1$.

B. Performance of Spectrally-Encoded Spread-Time UWB CDMA in the Presence of NBI

To demonstrate the narrowband interferences suppression ability of spectrally-encoded ST-CDMA, we consider a multi-user system in which a single zero mean stationary Gaussian partial band jammer with power spectral density $S_J(f) = \begin{cases} N_J/2 & |f \pm f_J| \leq W_J/2 \\ 0 & \text{o.w.} \end{cases}$ is present.

Fig. 6 shows the multi-user performance of the system both in the presence of NBI and after its cancellation, for $\rho \triangleq W_J/\Omega$ equal to 1 and 10, and for two different values of $SIR = \frac{E_0/T}{N_J W_J}$. The worst case condition that jammer's central frequency f_J is located at the spectral peak of the signal (f_m) is assumed. The good agreement between the simulation results and the approximations, especially as K gets large is apparent. We also notice the well pronounced dependence of the performance on the NBI bandwidth after its suppression. When the jammer is present the performance

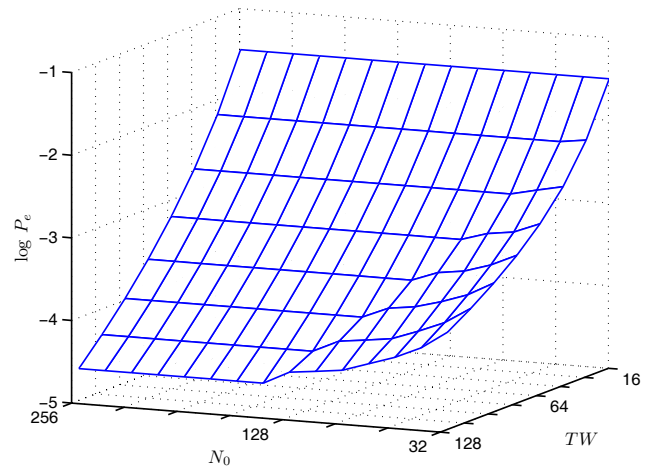


Fig. 5. Performance of the SE/ST CDMA technique versus time-bandwidth product and spectral code lengths for $K = 8$, based on the approximation (14).

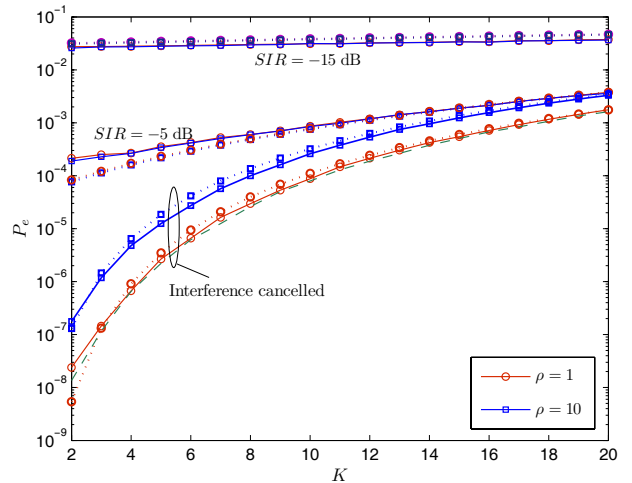


Fig. 6. Multi-user performance of the SE/ST CDMA technique in the presence and after the cancellation of NBI. Solid lines: Monte-Carlo simulation, dotted lines: approximation, dashed line: no interference present.

is solely determined by the total interference power and its dependence on ρ is intangible. Furthermore, we observe that when the multi-access noise increases if the interferer is not very strong and if ρ is large, its cancellation may not be of much an advantage.

The same concept is more clearly presented in Fig. 7. In this figure the performance is plotted as a function of the jammer central frequency for $K = 8$. The amount of BER improvement after the interference suppression highly depends on the jammer central frequency, jammer bandwidth, and jammer power. As can be noticed from the figure, in some cases (i.e., a quite wideband and weak jammer) the NBI cancellation may even worsen the system performance as a result of the significant reduction in the desired signal energy.

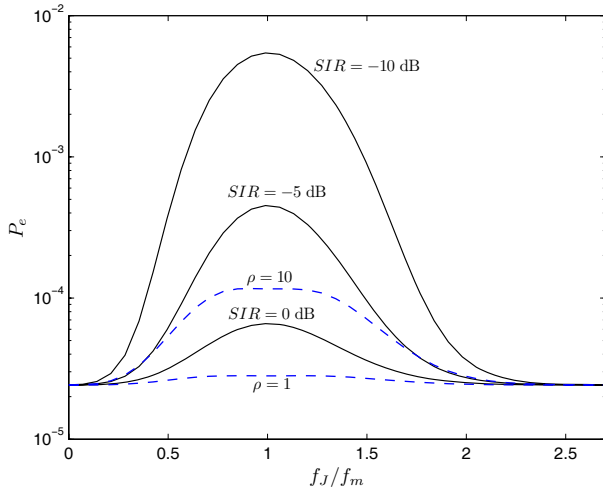


Fig. 7. Performance of the SE/ST CDMA technique in the presence and after the suppression of NBI vs. the jammer's central frequency normalized to f_m , for different values of jammer's bandwidth and power. Solid lines: before cancellation, dashed lines: after cancellation.

VI. CONCLUSION

In this paper we studied the performance of spectrally-encoded spread-time CDMA in UWB multiple-access systems. After investigating the statistical properties of the encoded pulse train, we evaluated the multiple-access performance of this technique in realistic UWB channels, both semi-analytically and through a simple approximation which proved to be in good agreement with numerical results. We also showed that the spectrally-encoded spread-time UWB system can easily overcome one of the major challenges of UWB technology, namely, coexistence with nearby narrow-band interferers. The effect of variations of the main system parameters and some of the relevant trade-offs were also investigated by numerical results. The results of this paper indicate the importance of the SE/ST modulation technique in an UWB CDMA communications system.

APPENDIX A

Let $s(t) = \sum_n a_n p(t - nT)$, where $p(t) = g(t) * pn(t)$, with $pn(t)$ being the inverse Fourier transform of the spectral code $PN(f)$. We have

$$\begin{aligned} R_s(t, t + \tau) &= \mathbb{E}\{s(t)s^*(t + \tau)\} \\ &= \mathbb{E}\left\{\sum_n \sum_m a_n a_m^* p(t - nT)p^*(t + \tau - mT)\right\} \end{aligned} \quad (23)$$

With $PN(f) = \sum_{k=-N_0/2}^{N_0/2-1} c_k r_\Omega(f - k\Omega)$, and noting that for i.i.d. ± 1 data sequence, $\mathbb{E}\{a_n a_m\} = \delta_{mn}$, the right hand side of (23) can be written as

$$\begin{aligned} \mathbb{E}\left\{\sum_n p(t - nT)p^*(t + \tau - nT)\right\} &= \mathbb{E}\left\{\sum_n \iint G(f)PN(f)G^*(f')PN^*(f')e^{j2\pi(t-nT)f}e^{-j2\pi(t+\tau-nT)f'}dfdf'\right\} = \\ &= \iint G(f)G^*(f')\sum_{k,k'=-N_0/2}^{N_0/2-1}\mathbb{E}\{c_k c_{k'}^*\}r_\Omega(f - k\Omega)r_\Omega(f' - k'\Omega)e^{j2\pi t(f-f')}e^{-j2\pi\tau f'}\sum_n e^{-j2\pi nT(f-f')}dfdf' \end{aligned} \quad (24)$$

As in [10], we choose $c_k = e^{jn_k\pi/2}$, where n_k takes on the values 0, 1, 2 or 3 with equal probability, so $\mathbb{E}\{c_k c_{k'}^*\} = \delta_{kk'}$ and $\mathbb{E}\{c_k c_{k'}\} = 0$, and with a use of Poisson's sum formula, (24) simplifies to

$$\begin{aligned} &\frac{1}{T}\sum_{k=-N_0/2}^{N_0/2-1}\iint G(f)G^*(f')r_\Omega(f - k\Omega)r_\Omega(f' - k\Omega)e^{j2\pi t(f-f')}e^{-j2\pi\tau f'}\sum_n \delta(f - f' - \frac{n}{T})dfdf' \\ &= \frac{1}{T}\sum_{k=-N_0/2}^{N_0/2-1}\sum_{n=-\infty}^{\infty}\int G(f)G^*(f - \frac{n}{T})r_\Omega(f - k\Omega)r_\Omega(f - \frac{n}{T} - k\Omega)e^{j2\pi t\frac{n}{T}}e^{-j2\pi\tau(f - \frac{n}{T})}df \end{aligned} \quad (25)$$

Using the fact that $r_\Omega(f - k\Omega)r_\Omega(f - \frac{n}{T} - k\Omega)$ is nonzero only for $|n| < T\Omega$, we have

$$\begin{aligned} R_s(t, t + \tau) &= \frac{1}{T}\int |G(f)|^2 e^{-j2\pi f\tau}df \\ &+ \frac{1}{T}\sum_{k=-N_0/2}^{N_0/2-1}\sum_{n=1}^{\lfloor T\Omega \rfloor}\left\{\int G(f)G^*(f - \frac{n}{T})r_{\Omega - \frac{n}{T}}(f - \frac{n}{T} - k\Omega)e^{j2\pi t\frac{n}{T}}e^{-j2\pi\tau(f - \frac{n}{T})}df + \right. \\ &\left. \int G(f)G^*(f + \frac{n}{T})r_{\Omega - \frac{n}{T}}(f - k\Omega)e^{-j2\pi t\frac{n}{T}}e^{-j2\pi\tau(f + \frac{n}{T})}df\right\} \end{aligned} \quad (26)$$

and if $G(f)$ is real, i.e., if $g(t)$ is real and even, a change of variable in (26) gives

$$\begin{aligned} R_s(t, t + \tau) &= \frac{1}{T}\int |G(f)|^2 e^{-j2\pi f\tau}df + \\ &\frac{2}{T}\sum_{n=1}^{\lfloor T\Omega \rfloor}\cos[\frac{2\pi n}{T}(t + \frac{\tau}{2})]\int G(f + \frac{n}{2T})G(f - \frac{n}{2T})r_{\Omega - \frac{n}{T}}(f - \frac{n}{2T} - k\Omega)e^{-j2\pi\tau f}df \end{aligned} \quad (27)$$

Using the Parseval's theorem in the last integral and noting that

$$\begin{aligned} &\mathcal{F}_\tau^{-1}\left\{\sum_{k=-N_0/2}^{N_0/2-1}r_{\Omega - \frac{n}{T}}(f - \frac{n}{2T} - k\Omega)\right\} \\ &= \mathcal{F}_\tau^{-1}\left\{r_{\Omega - \frac{n}{T}}(f - \frac{n}{2T})\right\}\sum_{k=-N_0/2}^{N_0/2-1}e^{j2\pi k\Omega\tau} \\ &= \frac{\sin(\Omega - n/T)\pi\tau}{\pi\tau}\frac{\sin\pi N_0\Omega\tau}{\sin\pi\Omega\tau} \end{aligned} \quad (28)$$

where $\mathcal{F}_\tau^{-1}\{\cdot\}$ denotes the inverse Fourier transform with τ as the argument, yields (4).

APPENDIX B

We first derive expressions for the mean and variance of the random variable $x = \sigma_i^2 + \sigma_n^2$. From the channel model described in section III, the channel coefficients can be written as $\alpha_l^{(j)} = b_l^{(j)}|\alpha_l^{(j)}|$. The $b_l^{(j)}$'s are equiprobable ± 1 random variables which are independent for different multipath components and different users. Hence

$$\mathbb{E}\{b_l^{(j)}b_{l'}^{(j)}b_i^{(j')}b_{i'}^{(j')}\} = \delta_{ll'}\delta_{ii'} \quad (29)$$

for $j \neq j'$, and for $j = j', j = 1, \dots, K$, we have

$$\mathbb{E}\{b_l^{(j)}b_{l'}^{(j)}b_i^{(j)}b_{i'}^{(j)}\} = \begin{cases} 1 & l = l', i = i' \\ 1 & l = i, l' = i' \\ 1 & l = i', l' = i \\ 0 & \text{otherwise} \end{cases} \quad (30)$$

From (10) and (29), and averaging over the delay of the first multipath components (15) is easily obtained.

Noting that

$$\sigma_x^2 = \mathbb{E}\{(\sigma_i^2)^2\} + \mathbb{E}\{(\sigma_n^2)^2\} + 2\mathbb{E}\{\sigma_i^2\sigma_n^2\} - \mu_x^2 \quad (31)$$

to compute the variance of x we first find $\mathbb{E}\{(\sigma_i^2)^2\}$. Squaring (10), averaging over $b_l^{(j)}$'s using (29) and (30), applying the assumption of resolvable multipath components, i.e., $|\tau_l^{(j)} - \tau_{l'}^{(j)}| \geq T_p$, $l \neq l'$, and noting that $R_{\bar{s}(j)}(t_1, t_2)$ is negligible for $|t_1 - t_2| > T_p$, gives

$$\begin{aligned} \mathbb{E}\{(\sigma_i^2)^2\} &= \mathbb{E}\{\|\alpha^{(1)}\|^4\} + \sum_{j=2}^K \mathbb{E}\{\|\alpha^{(j)}\|^2\}^2 \\ &+ 2 \sum_{j=2}^K \sum_{l=1}^L \sum_{l'=1, l' \neq l}^L \mathbb{E}\{|\alpha_l^{(1)}|^2 |\alpha_{l'}^{(1)}|^2\} \\ &+ \sum_{i=1}^{L_p^{(j)}} \mathbb{E}\{|\alpha_i^{(j)}|^2 |\alpha_{i+l-l'}^{(j)}|^2\} R_{\bar{s}(j)}^2(\tau_l^{(1)} - \tau_i^{(j)}, \tau_{l'}^{(1)} - \tau_{i'}^{(j)}) \end{aligned} \quad (32)$$

whence after averaging out the delays and substitution in (31), (16) is obtained. The same procedure, when applied to the random variable $x_1 = \mathbb{E}\{j_m^2 |\alpha^{(1)}\} + \sigma_i^2 + \sigma_n^2$, gives (22).

REFERENCES

- [1] S. Roy, J. R. Foerster, V. S. Somayazulu, and D. G. Leeper, "Ultrawideband radio design: the promise of high-speed, short-range wireless connectivity," *Proc. IEEE*, vol. 92, no. 2, pp. 295-311, Feb. 2004.
- [2] R. C. Qiu, H. Liu, and X. Shen, "Ultra-wideband for multiple access communications," *IEEE Commun. Mag.*, vol. 43, no. 2, pp. 80-87, Feb. 2005.
- [3] L. Yang and G. B. Giannakis, "Ultra-wideband communications: an idea whose time has come," *IEEE Signal Processing Mag.*, vol. 21, no. 6, pp. 26-54, Nov. 2004.
- [4] M. G. Shayesteh, J. A. Salehi, and M. Nasiri-Kenari, "Spread-time CDMA resistance in fading channels," *IEEE Trans. Wireless Commun.*, vol. 2, no. 3, pp. 446-458, May 2003.
- [5] M. Farhang and J. A. Salehi, "Spread-time/time-hopping UWB CDMA communication systems," in *Proc. IEEE ISCT Conf.*, Japan, Oct. 2004.
- [6] C. da Silva and L. B. Milstein, "Spectral-encoded UWB communication systems: real-time implementation and interference suppression," *IEEE Trans. Commun.*, vol. 53, no. 8, pp. 1391-1401, Aug. 2005.

- [7] J. Bellorado *et al.*, "Coexistence of ultra-wideband systems with IEEE-802.11a wireless LANs," in *Proc. IEEE GLOBECOM*, pp. 410-414, Dec. 2003.
- [8] M. Hamalainen, *et al.*, "On the UWB system coexistence with GSM900, UMTS/WCDMA, and GPS," *IEEE J. Select. Areas Commun.*, vol. 20, no. 9, pp. 1712-1721, Dec. 2002.
- [9] J. A. Salehi, A. M. Weiner, and J. P. Heritage, "Coherent ultrashort light pulse code-division multiple access communication systems," *J. Lightwave Technol.*, vol. 8, no. 3, pp. 478-491, Mar. 1990.
- [10] P. M. Crespo, M. L. Honig, and J. A. Salehi, "Spread-time code division multiple access," *IEEE Trans. Commun.*, vol. 43, no. 6, pp. 2139-2148, June 1995.
- [11] M. G. Shayesteh, M. Nasiri-Kenari, and J. A. Salehi, "Spread-time CDMA performance with and without windowing," in *Proc. IEEE Personal, Indoor and Mobile Radio Commun. (PIMRC)*, vol. 3, Sept. 2002, pp. 1166-1170.
- [12] J. R. Foerster, "The performance of a direct-sequence spread ultrawideband system in the presence of multipath, narrowband interference, and multiuser interference," in *Proc. IEEE Conf. Ultrawideband Syst. Technol.*, 2002, pp. 87-91.
- [13] J. M. Wozencraft and I. M. Jacobs, *Principles of Communications Engineering*. Wiley, 1965.
- [14] D. Cassioli, M. Z. Win, and A. F. Molisch, "The ultrawide bandwidth indoor channel: From statistical model to simulations," *IEEE J. Select. Areas Commun.*, vol. 20, no. 6, pp. 1247-1257, Aug. 2002.
- [15] L. J. Greenstein, S. S. Ghassemzadeh, S.-C. Hong, and V. Tarokh, "Comparison study of UWB indoor channel models," *IEEE Trans. Wireless Commun.*, vol. 6, no. 1, pp. 128-135, Jan. 2007.
- [16] T. Q. S. Quek and M. Z. Win, "Analysis of UWB transmitted-reference communication systems in dense multipath channels," *IEEE J. Select. Areas Commun.*, vol. 23, no. 9, pp. 1863-1874, Sept. 2005.
- [17] A. F. Molisch, J. R. Foerster, and M. Pendergrass, "Channel models for ultrawideband personal area networks," *Wireless Commun.*, vol. 10, no. 6, pp. 14-21, Dec. 2003.
- [18] J. Proakis, *Digital Communications*, 4th edition. McGraw Hill, 2001.
- [19] M. Z. Win, G. Chrisikos, and N. R. Sollenberger, "Performance of RAKE reception in dense multipath channels: implications of spreading bandwidth and selection diversity order," *IEEE J. Select. Areas Commun.*, vol. 18, no. 8, pp. 1516-1525, Aug. 2000.
- [20] Y. Ishiyama and T. Ohtsuki, "Performance comparison of UWB-IR using RAKE receivers in UWB channel models," in *Proc. IEEE Conf. Ultrawideband Syst. and Technol.*, 2004, pp. 226-230.
- [21] D. Cassioli, M. Z. Win, F. Vatalaro, and A. F. Molisch, "Performance of low-complexity RAKE reception in a realistic UWB channel," in *Proc. IEEE Int. Conf. Comm. (ICC)* 2002, pp. 763-767.
- [22] M. C. Jeruchim, P. Balaban, and K. S. Shanmugan, *Simulation of Communication Systems*, 2nd ed. Kluwer Academic, 2000.
- [23] First report and order, revision of part 15 of the commission's rules regarding ultra-wideband transmission systems Washington, DC: FCC, ET Docket 98-153, 2002.
- [24] J. M. Holtzman, "A simple, accurate method to calculate spread-spectrum multiple-access error probabilities," *IEEE Trans. Commun.*, vol. 40, no. 3, pp. 461-464, Mar. 1992.
- [25] K. B. Letaief, "Efficient evaluation of the error probabilities of spread-spectrum multiple-access communications," *IEEE Trans. Commun.*, vol. 45, no. 2, pp. 239-246, Feb. 1997.
- [26] Y. C. Yoon, "A simple and accurate method of probability of bit error analysis for asynchronous band-limited DS-SS systems," *IEEE Trans. Commun.*, vol. 50, no. 4, pp. 656-663, Apr. 2002.
- [27] J. M. Holtzman, "On using perturbation analysis to do sensitivity analysis: derivatives vs. differences," in *Proc. IEEE Conf. Decision Control*, pp. 2018-2023, Dec. 1989.
- [28] P. Billingsley, *Probability and Measure*. Wiley, 1979.



Technology, Sapporo, Japan.

Mahmoud Farhang (S'06) received the B.Sc. degree (with highest honors) from Shiraz University, Shiraz, Iran, in 2002 and M.Sc. degree from Sharif University of Technology, Tehran, Iran, in 2004, both in Electrical Engineering. He is now working toward Ph.D. at Sharif University of Technology. His current research interests include statistical communication theory and ultrawideband optical and radio communications. He is the coreipient of the IEEE's Best Paper Award in 2004 from the International Symposium on Communications and Information



Jawad A. Salehi (M'84-SM'07) was born in Kazemian, Iraq, on December 22, 1956. He received the B.S. degree from the University of California, Irvine, in 1979, and the M.S. and Ph.D. degrees from the University of Southern California (USC), Los Angeles, in 1980 and 1984, respectively, all in electrical engineering. He is currently a Full Professor at the Optical Networks Research Laboratory (ONRL), Department of Electrical Engineering, Sharif University of Technology (SUT), Tehran, Iran, where he is also the Co-Founder of

the Advanced Communications Research Institute (ACRI). From 1981 to 1984, he was a Full-Time Research Assistant at the Communication Science Institute, USC. From 1984 to 1993, he was a Member of Technical Staff of the Applied Research Area, Bell Communications Research (Bellcore), Morristown, NJ. During 1990, he was with the Laboratory of Information and Decision Systems, Massachusetts Institute of Technology (MIT), Cambridge, as a Visiting Research Scientist. From 1999 to 2001, he was the Head of the Mobile Communications Systems Group and the Co-Director of the Advanced and Wideband Code-Division Multiple Access (CDMA) Laboratory, Iran

Telecom Research Center (ITRC), Tehran. From 2003 to 2006, he was the Director of the National Center of Excellence in Communications Science, Department of Electrical Engineering, SUT. He is the holder of 12 U.S. patents on optical CDMA. His current research interests include optical multiaccess networks, optical orthogonal codes (OOC), fiber-optic CDMA, femtosecond or ultrashort light pulse CDMA, spread-time CDMA, holographic CDMA, wireless indoor optical CDMA, all-optical synchronization, and applications of erbium-doped fiber amplifiers (EDFAs) in optical systems. Prof. Salehi is an Associate Editor for Optical CDMA of the IEEE TRANSACTIONS ON COMMUNICATIONS since May 2001. In September 2005, he was elected as the Interim Chair of the IEEE Iran Section. He was the recipient of several awards including the Bellcore's Award of Excellence, the Nationwide Outstanding Research Award from the Ministry of Science, Research, and Technology in 2003, and the Nation's Highly Cited Researcher Award in 2004. He is among the 250 preeminent and most influential researchers worldwide in the Institute for Scientific Information (ISI) Highly Cited in the Computer-Science Category. He is the corecipient of the IEEE's Best Paper Award in 2004 from the International Symposium on Communications and Information Technology, Sapporo, Japan.